

# Using Synthetic Aperture Radar to Define Spring Breakup on the Kuparuk River, Northern Alaska

ANGELICA L. FLOYD,<sup>1,2</sup> ANUPMA PRAKASH,<sup>1</sup> FRANZ J. MEYER,<sup>1</sup> RÜDIGER GENS<sup>1,3</sup> and ANNA LILJEDAHL<sup>4</sup>

(Received 12 September 2013; accepted in revised form 14 February 2014)

**ABSTRACT.** Spring runoff measurements of Arctic watersheds are challenging given the remote location and the often dangerous field conditions. This study combines remote sensing techniques and field measurements to evaluate the applicability of synthetic aperture radar (SAR) to defining spring breakup of the braided lower Kuparuk River, North Slope, Alaska. A statistical analysis was carried out on a time series (2001–10) of SAR images acquired from the European Remote Sensing Satellite (ERS-2) and the Canadian RADARSAT satellite, as well as on measured runoff. On the basis of field information, the SAR images were separated into pre-breakup, breakup, and post-breakup periods. Three variables were analyzed for their suitability to bracket the river breakup period: image brightness, variance in brightness over the river length, and a sum of rank order change analysis. Variance in brightness was found to be the most reliable indicator. A combined use of that variance and sum of rank order change appeared promising when enough images were available. The temporal resolution of imagery served as the major limitation in constraining the timing of the hydrologic event. Challenges associated with spring runoff monitoring and the sensitive nature of SAR likely resulted in an earlier detection of surficial changes by the remote sensing technique compared to the field runoff observations. Given a sufficient temporal resolution, SAR imagery has the potential to improve the spatiotemporal monitoring of Arctic watersheds for river breakup investigations.

**Key words:** breakup, SAR, radar, river ice, Kuparuk River, Alaska, remote sensing

**RÉSUMÉ.** La mesure de l'écoulement printanier des bassins hydrographiques de l'Arctique n'est pas facile à réaliser en raison de l'éloignement ainsi qu'en raison des conditions souvent dangereuses qui ont cours sur le terrain. Cette étude fait appel à des techniques de télédétection de même qu'aux mesures prises sur le terrain pour évaluer l'applicabilité du radar à synthèse d'ouverture SAR pour définir la débâcle printanière de la basse rivière Kuparuk anastomosée sur la North Slope de l'Alaska. L'analyse statistique d'une série temporelle (2001-2010) d'images SAR acquises à partir du satellite européen de télédétection (ERS-2) et du satellite canadien RADARSAT ainsi que des écoulements mesurés a été effectuée dans le cadre de cette étude. D'après les renseignements recueillis sur le terrain, les images SAR ont été divisées en fonction de la période précédant la débâcle, de la période de la débâcle même et de la période suivant la débâcle. Trois variables ont été analysées afin de déterminer si elles permettaient d'isoler la période de la débâcle de la rivière, soit la luminance de l'image, la variance de la luminance en fonction de la longueur de la rivière et la somme de l'analyse des changements de classement suivant le rang. La variance de la luminance s'est avérée l'indicateur le plus fiable. L'utilisation conjointe de cette variance et de la somme des changements de classement suivant le rang s'avéraient prometteuse lorsque le nombre d'images était suffisant. La résolution temporelle de l'imagerie a constitué la plus grande limitation pour contraindre la temporisation de l'événement hydrologique. Les défis liés à la surveillance de l'écoulement printanier et la nature sensible du SAR ont vraisemblablement donné lieu à la détection précoce des changements superficiels au moyen de la technique de télédétection comparativement aux observations mêmes de l'écoulement printanier. Moyennant une résolution temporelle suffisante, l'imagerie SAR pourrait permettre d'améliorer la surveillance spatiotemporelle des bassins hydrographiques de l'Arctique en vue de l'étude des débâcles printaniers.

**Mots clés :** débâcle, SAR, radar, glace de rivière, rivière Kuparuk, Alaska, télédétection

Traduit pour la revue *Arctic* par Nicole Giguère.

---

<sup>1</sup> Geophysical Institute, University of Alaska Fairbanks, 903 Koyukuk Drive, Fairbanks, Alaska 99709, USA

<sup>2</sup> Corresponding author: [angelica.floyd@alaska.edu](mailto:angelica.floyd@alaska.edu)

<sup>3</sup> Alaska Satellite Facility, University of Alaska Fairbanks, 903 Koyukuk Drive, Fairbanks, Alaska 99709, USA

<sup>4</sup> Water and Environmental Research Center, University of Alaska Fairbanks, 306 Tanana Loop, Fairbanks, Alaska 99709, USA and International Arctic Research Center, University of Alaska Fairbanks, 903 Koyukuk Drive, Fairbanks, Alaska 99709, USA

## INTRODUCTION

Arctic rivers control freshwater export into the Arctic Ocean and influence sediment transport, oceanic processes, and sea ice (Steele et al., 1996; Broecker, 1997; Peterson et al., 2002; Rahmstorf, 2002). Changes to the timing or volume of river discharge can affect the extent of the sea ice cover, and therefore, ocean-atmosphere energy exchanges (Searcy et al., 1996). The seasonality of Arctic river processes is also very important for local residents. For example, an earlier breakup influences availability of freshwater and fish habitat (Jeffries et al., 2005; Prowse et al., 2006) and generally results in a shorter tundra travel season. Impacts of ice jams and subsequent flooding affect infrastructure development plans for transportation and industry (Prowse and Beltaos, 2002). While the hydrology of Arctic rivers clearly has ecological and socio-economic impacts, the logistical challenges posed by this vast and remote area make ground-based monitoring extremely difficult.

Few rivers in the Arctic have been gauged, and even fewer are actively measured (Bring and Destouni, 2009). Previous research on river ice using SAR images has focused heavily on classifying river ice types (Weber et al., 2003; Gauthier et al., 2006; Unterschultz et al., 2009) and inferring ice cover roughness and thickness (Jasek et al., 2003; Mermoz et al., 2013). Pavelsky and Smith (2004) used optical images from the Moderate Resolution Imaging Spectroradiometer (MODIS) and Advanced Very High Resolution Radiometer (AVHRR) to estimate temporal patterns in ice breakup along Arctic rivers. There have been limited efforts to define the timing of river breakup using radar remote sensing techniques. These include the work by Gauthier et al. (2010), who used a radar-based approach to map river ice in Canada during both freeze-up and breakup periods. Jeffries et al. (2005) used radar images to detect the fractures that mark the start of the mechanical breakup of river ice in spring. These studies demonstrated that SAR data are sensitive to changes in surface characteristics of river ice and can capture the rather dramatic changes that occur during breakup. However, these earlier studies were carried out on very large rivers, relied solely on the brightness value or textural variations in the SAR images, and were limited by visual image interpretation guided by the user's field experience. In this paper, we statistically analyze a time-series of SAR data and present an approach to bracketing the period of river breakup and monitoring an Arctic river. For our purposes, we define river breakup as the swift initial rise in discharge forming a distinctive large peak on the hydrograph after a period of dormancy during the winter months.

Typically, open water appears during the breakup period, to the extent that a river may become completely ice-free. However, in the Lower Kugaruk River (our study area), a peak in the hydrograph can occur when there is still extensive ice in the river. Therefore, the breakup period is marked by the presence of open water with chunks of floating ice. We chose the Kugaruk River watershed in northern Alaska for testing because this site is well researched: it has

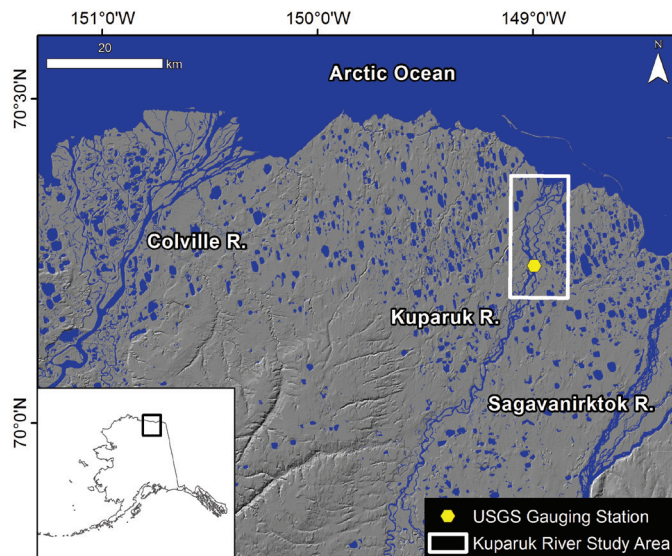


FIG. 1. Location of the Lower Kugaruk River study area. The background image is a shaded relief map derived from a digital elevation model available through the National Elevation Dataset.

two monitored gauging stations and an excellent record of hydrologic field data (Kane and Hinzman, 2012). Our study demonstrates that the statistical method works well even for narrower rivers, such as the lower Kugaruk, where the channel width is on the order of 30 to 100 m.

## STUDY AREA

The Lower Kugaruk River study area, depicted in Figure 1, is bounded by latitudes  $70^{\circ}25'7''$  and  $70^{\circ}14'1''$  N and longitudes  $148^{\circ}59'16''$  and  $149^{\circ}1'11''$  W. It includes one gauging station (station ID 15896000) established in 1973 and monitored by the U.S. Geological Survey (USGS). A second gauging station in the headwaters of the Kugaruk River watershed (outside the region of interest for this study) is monitored by the Water and Environmental Research Center, University of Alaska Fairbanks.

The Kugaruk River watershed (8140 km<sup>2</sup>) slopes downward for nearly 250 km from the northern foothills of the Brooks Range to the Arctic Coastal Plain and the Arctic Ocean. Although some North Slope rivers do have a contribution from glacial meltwater, the Kugaruk River basin is unglaciated (Kane et al., 2000). The Lower Kugaruk River is braided and underlain with continuous permafrost, with depths that can exceed 600 m (Osterkamp and Payne, 1981). The topography is flat near the coast and dotted with many lakes, which increase in frequency closer to the ocean (Shiklomanov and Nelson, 2002). The vegetation is shrublands and wet tussock tundra, and 83% of the coastal plain is categorized as wetlands, resulting in a large capacity for surficial storage (Kane et al., 2000).

The coastal plain has cold winters and cool summers with winds from the Arctic Ocean. The mean annual air temperature at the lower Kugaruk River is about  $-12^{\circ}\text{C}$ ,

with temperatures rising above freezing only from June to September. Annual precipitation at the northernmost Arctic Coastal Plain averages 173 mm (Liljedahl et al., 2011) and tends to be greatest in July and August (Rovaneck et al., 1996). The entire Kuparuk River watershed is snow covered for seven to nine months of the year, and approximately 50% of the precipitation falls as snow (Zhang et al., 1996).

One unique trait of Arctic rivers is the extreme seasonality of flow. During the long winter months, the Kuparuk River is frozen and limited discharge (if any) occurs from groundwater springs that form isolated aufeis (Kane et al., 1991; Yoshikawa et al., 2007). Spring runoff is the major hydrologic event of the year, as a snowpack that has accumulated for eight to nine months rapidly melts (Kane et al., 1997, 2000, 2003). The ablation period typically lasts for 7–14 days (Kane et al., 1997). McNamara et al. (1998) found that snowmelt provides up to 80% of the annual runoff from the Kuparuk River. Summer precipitation is also important in causing increased runoff from the Kuparuk River because the underlying permafrost limits the potential subsurface storage of water (Kane et al., 2003, 2008).

## DATA SOURCES

This study is based on 61 spring and summer (May–July) SAR images from 2001–10 (data from the year 2002 were later removed from the analysis because of low temporal resolution) (Table 1). Data were collected from the Alaska Satellite Facility's RADARSAT-1 and ERS-2 archives. Both sensors are singularly polarized, RADARSAT-1 in HH polarization and ERS-2 in VV, and both sensors operate in C-band with microwave wavelengths of approximately 5.6 cm and 5.3 cm, respectively. Images from both sensors were calibrated and converted to Geotiff images with 12.5 m<sup>2</sup> pixels.

Hourly wind speeds were collected by the climate station located at the airport of Deadhorse, Alaska (station identifier PASC). Discharge information published by the USGS as daily measurements (USGS, 2012) were used for this study. A National Elevation Dataset digital elevation model provided by the USGS was also used.

## METHODS

### *SAR Sensitivity to River Ice Conditions*

In a SAR image, smooth open water surfaces act as specular reflectors: they scatter microwaves away from the sensor so that little backscatter is returned, which causes calm open water to have a dark appearance in SAR images (Weber et al., 2003). Ice can give either a bright or a dark response in SAR depending on the surface smoothness, dielectric constant, and water content (Rees, 2006).

If the ice surface is wet and rough, diffuse surface scattering occurs, and the ice surface will look relatively

TABLE 1. List of the 65 SAR granules used for analysis of the Lower Kuparuk River. Alaska Satellite Facility granule name and date of satellite acquisition are listed. R1 refers to RADARSAT 1 images and E2 refers to ERS 2 images. A = ascending and D = descending.

Granule	Date	Look angle	A/D
R1_29057_ST2_F273	5/29/01	27.2	D
E2_31961_STD_F273	5/31/01	22.9	D
R1_29249_ST3_F177	6/12/01	33.6	A
E2_32276_STD_F272	6/22/01	23.1	D
E2_32462_STD_F273	7/5/01	22.9	D
E2_36785_STD_F273	5/3/02	23.1	D
E2_37292_STD_F177	6/8/02	23.0	A
E2_37515_STD_F273	6/23/02	22.9	D
E2_37744_STD_F273	7/9/02	22.9	D
E2_42024_STD_F273	5/4/03	22.9	D
E2_42030_STD_F177	5/5/03	22.9	A
E2_42488_STD_F177	6/6/03	22.9	A
E2_42525_STD_F273	6/8/03	22.9	D
E2_42797_STD_F273	6/27/03	23.0	D
E2_47306_STD_F273	5/7/04	22.9	D
E2_47498_STD_F177	5/21/04	22.9	A
E2_47764_STD_F273	6/8/04	22.9	D
E2_47999_STD_F177	6/25/04	22.9	A
E2_48036_STD_F273	6/27/04	23.0	D
E2_48042_STD_F177	6/28/04	22.9	A
E2_48265_STD_F273	7/13/04	22.9	D
E2_48271_STD_F177	7/14/04	22.9	A
E2_52545_STD_F273	5/8/05	22.7	D
E2_52551_STD_F177	5/9/05	22.9	A
R1_49672_ST6_F176	5/11/05	43.7	A
R1_49729_FN1_F176	5/15/05	37.9	A
E2_52817_STD_F273	5/27/05	22.9	D
E2_53052_STD_F177	6/13/05	22.9	A
E2_53275_STD_F273	6/28/05	22.9	D
R1_50515_ST3_F176	7/9/05	33.4	A
E2_53547_STD_F273	7/17/05	22.9	D
E2_57784_STD_F273	5/9/06	22.9	D
E2_58013_STD_F273	5/25/06	22.9	D
E2_58285_STD_F273	6/13/06	22.9	D
E2_58557_STD_F273	7/2/06	22.9	D
E2_58786_STD_F273	7/18/06	22.9	D
E2_58829_STD_F272	7/21/06	23.1	D
E2_63072_STD_F177	5/14/07	22.9	A
E2_63295_STD_F273	5/29/07	22.9	D
E2_63338_STD_F273	6/1/07	22.9	D
R1_60462_ST3_F176	6/5/07	33.3	A
E2_63530_STD_F177	6/15/07	22.9	A
E2_63573_STD_F177	6/18/07	22.9	A
R1_60719_ST1_F177	6/23/07	22.1	A
E2_63796_STD_F274	7/3/07	22.9	D
E2_68305_STD_F273	5/13/08	22.7	D
E2_68311_STD_F177	5/14/08	23.1	A
E2_68348_STD_F273	5/16/08	22.7	D
E2_68583_STD_F177	6/2/08	22.9	A
E2_68806_STD_F273	6/17/08	22.7	D
E2_68812_STD_F177	6/18/08	22.9	A
E2_68849_STD_F273	6/20/08	22.7	D
E2_73550_STD_F177	5/15/09	23.1	A
E2_73587_STD_F273	5/17/09	22.9	D
E2_73593_STD_F177	5/18/09	22.9	A
E2_73816_STD_F273	6/2/09	22.9	D
E2_73859_STD_F273	6/5/09	22.9	D
E2_74088_STD_F273	6/21/09	22.9	D
E2_78826_STD_F273	5/18/10	22.7	D
E2_78869_STD_F273	5/21/10	22.8	D
E2_79061_STD_F177	6/4/10	22.9	A
E2_79098_STD_F273	6/6/10	22.7	D
E2_79104_STD_F177	6/7/10	22.9	A
E2_79327_STD_F273	6/22/10	22.8	D
E2_79370_STD_F273	6/25/10	22.8	D

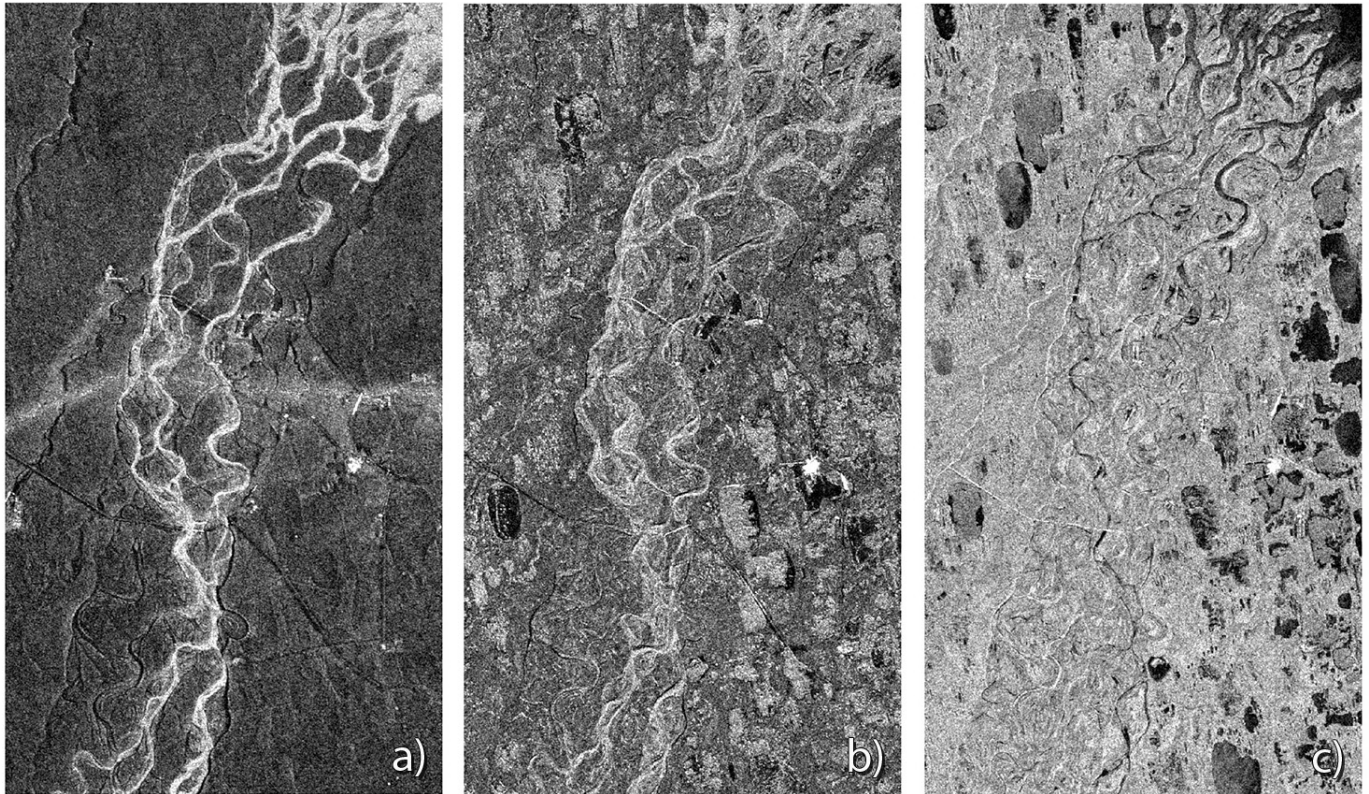


FIG. 2. ERS-2 images for the lower Kuparuk River acquired on (a) 27 May 2005, showing a bright river due to high backscatter; (b) 13 June 2005, showing variable brightness along the river several days after the peak of the spring runoff event; (c) 28 June 2005, showing a typical low backscatter response from calm, free-flowing water in the river channel.

bright in the SAR image. If the ice is smooth and wet (possibly from saturated snow or meltwater on the surface), it behaves as a specular reflector, similarly to open water, and appears dark in the SAR image (Unterschultz et al., 2009). Volume scattering occurs when the snow or ice layer is dry and microwaves penetrate the surface only to be scattered by discontinuities within the ice matrix, such as cracks, air bubbles, sediment, and pockets of liquid water. Volume scattering can lead to significant backscatter, depending on how inhomogeneous the ice pack is (Unterschultz et al., 2009). If ice is frozen to the ground, backscatter is influenced by the changes in material properties (particularly dielectric constant) between ice and rock (Weeks et al., 1978; Jeffries et al., 2005), though the Kuparuk River likely does not freeze to the bottom of the channel (Best et al., 2005). In this study we investigate whether an analysis of signal variations in a time-series of SAR images can identify the breakup of river ice, given the dramatically changing nature of the river's surficial properties during breakup and the sensitivity of SAR to these changes.

The radar brightness observed in a SAR image depends not only on surface properties, but also on a set of sensor parameters, such as the sensor's wavelength, incidence angle, and polarization. To minimize these influences, only C-band data with similar wavelength are used in this study, and differences in incidence angles were kept small (see Table 1). Minor incidence angle-related effects on image brightness were further mitigated using an existing digital

elevation model (see *Brightness* in next section). Polarization effects are also small, as most acquisitions were made in VV polarization and only a few acquisitions in HH polarization were added to achieve a higher temporal resolution. While, in principle, a change in backscatter response is expected in the HH and VV polarized signal, this difference is moderate for many surface scattering phenomena (see Van Zyl and Kim, 2011) and had no significant impact on the results of our study.

Figure 2 shows a set of three images from the study area with a variety of backscatter responses. Figure 2a shows a bright backscatter from large parts of the frozen river, as anticipated. Figure 2b is an example of spatially variable backscatter response due to confounding effects, even though this image was taken several days after the peak discharge on the hydrograph. Figure 2c is a typical backscatter response from a post-breakup image that is dominated by free water flow. The images demonstrate that backscatter is important, but not always the most dependable criterion for bracketing river breakup.

#### *SAR Data Processing and Statistical Analysis of Breakup Indicators*

Our study included three main steps: preprocessing of images, wind correction, and statistical analysis.

**Preprocessing:** Several image-processing steps were applied during preprocessing. First the ASF software

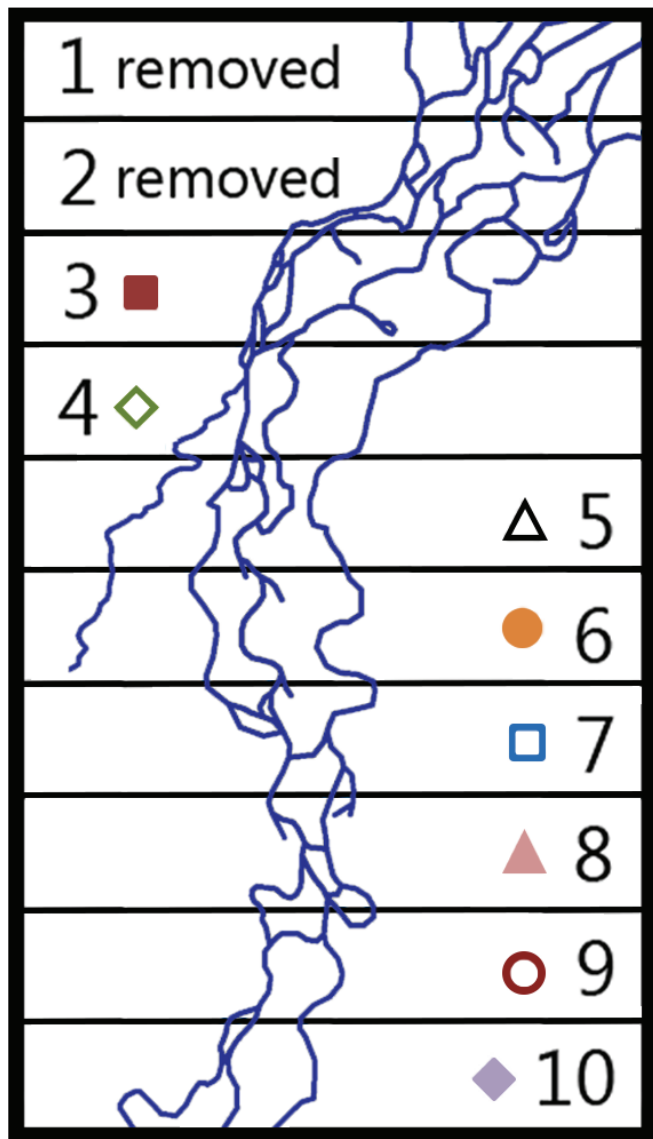


FIG. 3. The lower Kugaruk River study area was divided into 10 river segments for the statistical analysis. The symbols show how each segment is depicted on the graphs used for analysis.

package, MapReady, was used to geocode the SAR images to the WGS84 UTM Zone 6N map projection, resample all data to a pixel size of 12.5 m, rescale the image into sigma dB scale, and improve geolocation accuracy through Fast Fourier Transform (FFT) matching (Gens and Logan, 2003). MapReady was also used in combination with the available digital elevation model to mitigate some of the incidence angle effects in the observed image brightness values and to prepare images acquired at slightly different incidence angles for direct comparison. Then the river centerline was digitized using ESRI's ArcGIS software package, and pixels included within a 25 m buffer around the river centerline were extracted. This step ensured that only the river pixels were extracted without contamination from the surrounding land pixels.

**Wind Correction:** Wind is known to influence the backscatter response of water surfaces and has the potential

to affect the radar brightness signature. We therefore attempted to correct for wind effects by graphing wind speed against the mean brightness of the entire extracted river length and identifying the regression model that best fit the data. This method was adapted from Horstmann et al. (2003), who used SAR image brightness to measure global surface winds over oceans. For the regression analysis, wind measurements taken most closely to the time of image acquisition were plotted against the mean radar brightness along the river, and a linear least-squares regression was performed. We selected a linear regression model for wind correction since more complex models (quadratic, exponential) did not significantly improve the correlation between data and model.

Wind influence was investigated separately for each hydrological period (pre-breakup, breakup, and post-breakup), and the coefficients of determination ( $R^2$ ) for each linear regression were recorded. The regressions were statistically significant using the Pearson Product-Moment test at the 95% confidence level in both the pre-breakup and breakup periods. Hence, the estimated regression models were subtracted from the data to compensate for wind influence.

**Statistical Analysis:** For statistical analysis, the study area was divided into 10 sections of identical area (Floyd et al., 2012). Segmenting the river (Fig. 3) allowed local changes in the river surface to be captured, while still allowing for enough river pixels per segment to perform a statistical analysis. Each river segment had at least 30 pixels, which provided enough data to carry out a Gaussian analysis of the calculated mean values. Segments one and two were removed from the analysis because of possible deltaic and tidal influences.

We tested the applicability of three different parameters—segment brightness, brightness variance between river segments, and the sum of segment rank order changes—as indicators for river ice breakup.

**Brightness:** Radar brightness in images acquired at rather similar incidence angles is directly related to the physical properties of an imaged target and is therefore useful in analyzing changes in physical ice properties over time. As water and ice typically have different backscatter response (Mermoz et al., 2009), we used image segment brightness as the first possible breakup indicator. Mean river segment brightness in dB was plotted on the y-axis, and the date of image acquisition on the x-axis. Each of the eight river segments was labeled with its own unique symbol, so that the response of each river segment was evident in the plot of brightness values from dates of SAR acquisitions. River discharge data were plotted on a secondary y-axis, and the breakup flood event is illustrated as the first peak of the hydrograph curve (Fig. 4).

**Variance:** The variance reflects the spread of brightness values of the river segments in a particular image. A low variance along a river is anticipated when the river is either completely frozen or freely flowing with no ice. In contrast, just prior to and during breakup, a variable backscatter

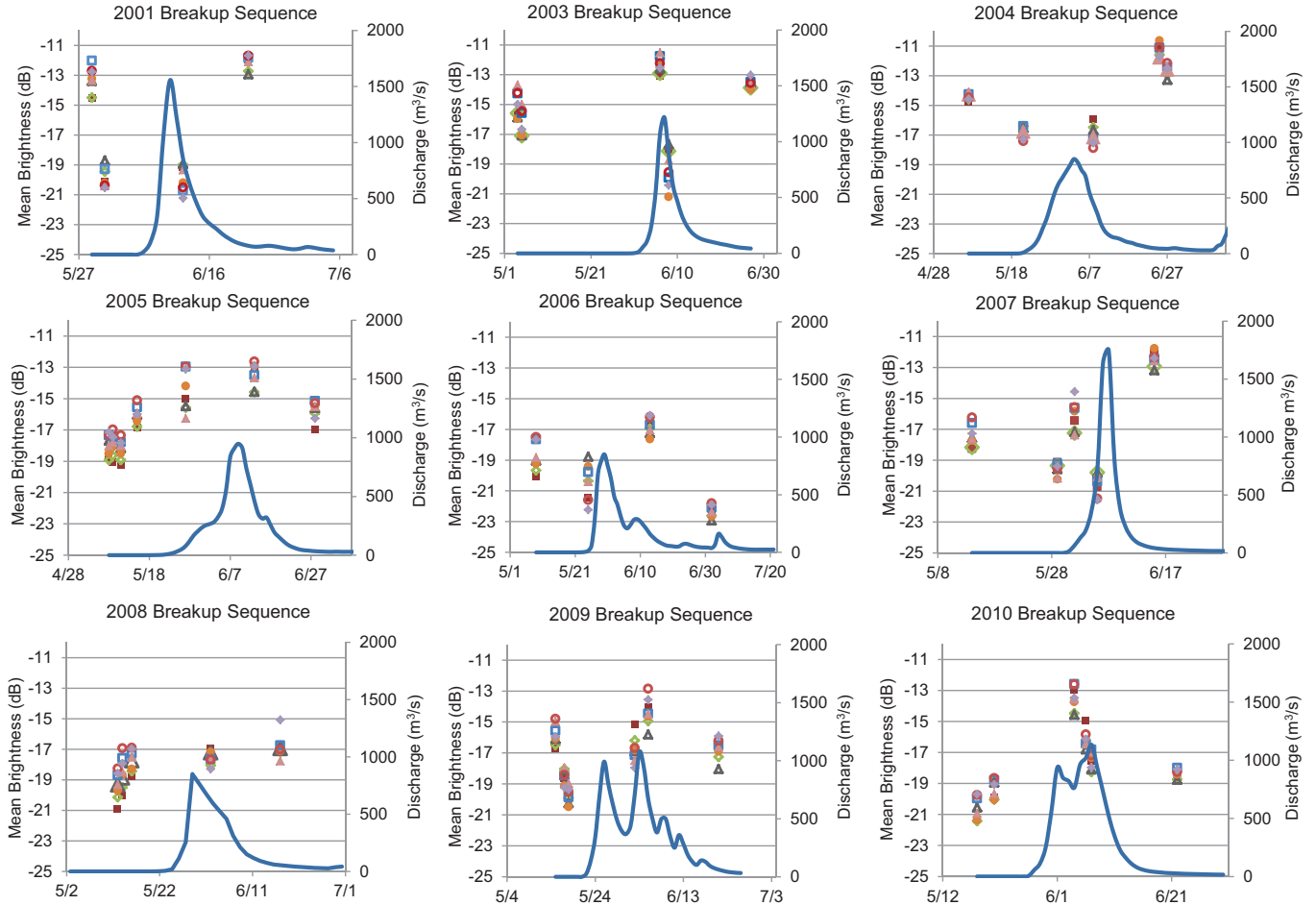


FIG. 4. Plots of river segment brightness for the years 2001 to 2010. Individual river segments are shown as separate symbols, which are located on the plot according to brightness (left y-axis). The blue line represents discharge over the time period and refers to the scale on the right y-axis. The year 2002 was omitted from the analysis.

response is anticipated because complex processes operating under variable combinations of ice and water in the river cause the river segments to respond differently. Therefore, we tested variance as another possible breakup indicator. Variance in the brightness of the river segments in each image was calculated, and the image date with the highest variance was highlighted (Table 2).

**Sum of Rank Order Change:** Following a similar rationale as in image variance, we established another possible breakup indicator called the sum of rank order change (SROC). SROC works on the assumption that the same river segment will show relatively little change in successive images during completely frozen no-flow conditions, or during homogenous full-flow river condition. However, just prior to breakup or during breakup, when ice is shifting, fracturing, melting, and flooding, significant changes in image brightness response will occur for the same image segment in successive images.

We calculated SROC in two steps. First the mean brightness of each segment was ranked on a scale of 1 (brightest) to 8 (darkest). If two segments had exactly the same mean brightness, they were assigned the same rank. The change in rank was calculated as:

$$|\text{segment}_n \text{image}_1 - \text{segment}_n \text{image}_2| = \Delta \text{rank}_{\text{segment}_n} \quad (1)$$

where  $\text{image}_1$  is the first date and  $\text{image}_2$  is the second in the chronological sequence and  $n$  is the specific river segment under consideration.

In the second step, the changes in rank calculated from equation 1 were summed to determine the SROC:

$$\text{SROC} = \sum_{n=1}^N \Delta \text{rank}_{\text{segment}_n} \quad (2)$$

Accordingly, a higher SROC value was anticipated to indicate a breakup period. As SROC requires an image pair for meaningful comparison of pre- and post-breakup conditions, it is important when using this indicator to have at least two pre-breakup images and two post-breakup images available.

## RESULTS AND DISCUSSION

The result of plotting all three breakup indicators for all river segments for the entire temporal sequence of SAR images (years 2001–10, excluding 2002) is shown in Figure 4. In addition to SAR-related information, the

TABLE 2. Variance of brightness between river segments for each SAR acquisition. Date with the highest variance in each year is in bold.

Year	Image date	Variance
2001	May 29	0.739
	May 31	0.431
	<b>June 12</b>	<b>0.782</b>
	June 22	0.232
2003	May 4	0.748
	May 5	0.797
	June 6	0.285
	<b>June 8</b>	<b>1.582</b>
	June 27	0.081
2004	May 7	0.035
	May 21	0.146
	<b>June 8</b>	<b>0.391</b>
	June 25	0.193
	June 27	0.125
2005	May 8	0.507
	May 9	0.471
	May 11	0.402
	May 15	0.350
	<b>May 27</b>	<b>1.743</b>
	June 13	0.571
	June 28	0.352
2006	May 9	0.984
	<b>May 25</b>	<b>1.404</b>
	June 13	0.270
	July 2	0.151
2007	May 14	0.500
	May 29	0.163
	<b>June 1</b>	<b>0.994</b>
	June 5	0.494
	June 15	0.198
2008	May 13	0.772
	<b>May 14</b>	<b>1.017</b>
	May 16	0.496
	June 2	0.197
	June 17	0.619
2009	May 15	0.464
	May 17	0.205
	May 18	0.237
	June 2	0.704
	<b>June 5</b>	<b>0.800</b>
	June 21	0.432
2010	May 18	0.554
	May 21	0.348
	<b>June 4</b>	<b>0.584</b>
	June 6	0.314
	June 22	0.102

hydrograph is also plotted on each graph and its corresponding discharge numbers are shown on the second y-axis on the right side of each plot (Fig. 4).

Average segment brightness (breakup indicator 1) is plotted using different symbols for each river segment. Image brightness varies greatly from image to image, with no clear relationship to the surficial characteristics of the river (Fig. 4). An example of this is the 2007 breakup sequence, which displays no correlation between

the brightness pattern and the hydrologic period. In most instances, overall brightness was not an effective indicator of river breakup. Note that the variation of radar brightness through the image time series did not correlate with the geometry of the image acquisition and was large even for images acquired in identical image geometries.

The variance of brightness along the river per image acquisition time (breakup indicator 2) can be inferred from the vertical spread of symbols per time step (Fig. 4, Table 2). Variance between river segments was frequently higher in images acquired during breakup than in images of frozen or completely open water conditions. Variance was highest during breakup in all years except 2008. This pattern is most clearly depicted in the 2003 and 2006 graphs, where the spread of brightness values for all river segments is greatest when the hydrograph shows a steep increase in discharge. Year 2008 is the only year in which the greatest variance does not correspond to the breakup event, but instead to the pre-breakup period. High pre-breakup variances are likely due to other confounding mechanisms associated with the breakup period, such as unusual snow redistribution or possibly a slight melting of surface ice under extended solar illumination conditions. However, we do not have field data to validate this interpretation.

The SROC (breakup indicator 3) values (Table 3) indicate that sometimes the segment response dramatically shifted during and after the breakup event.

SROC results are further highlighted in Figure 5, which is a close-up view of two days in the 2003 breakup sequence that is shown in full in Figure 4. As shown in this figure by the sequence of the symbols, the pattern or relative brightness response between two pre-breakup images is very similar. Therefore, this image pair exhibits a very low sum of rank order change.

To quantify whether or not the sum of rank order change analysis led to a successful bracketing of river breakup, we tried to identify significant breakup-induced increases in the sum of rank order change. For this study, an increase in the sum of rank order changes was considered significant if the change was 10 or higher. This was true for four years of the analyzed time series: 2003, 2005, 2008, and 2009. These years all have at least two pre-breakup images (one pre-breakup image pair). This SROC indicator yields useful results only if there is at least one pre-breakup image pair to compare to a breakup or post-breakup image pair. For this reason, the sum of rank order change analysis could not be performed for the year 2006, for which we were lacking pre-breakup data.

The combined results of analyses of all three breakup indicators are summarized in Table 4, which shows the overall success of each indicator for each year.

Brightness was not an effective breakup indicator for any year. This result indicates that there are likely several factors such as winds, wetness, and snow accumulation that can cause changes in brightness values and confound the backscatter analysis. Variance and SROC, however, do not measure absolute backscatter response, but are parameters

TABLE 3. Sum of rank order change for each image pair in all years in the temporal stack.

Year	Image pair	Sum of rank order $\Delta$
2001	May 29/May 31	27
	May 31/June 12	13
	June 12/June 22	31
2003	May 4/May 5	7
	May 5/June 6	7
	June 6/June 8	30
	June 8/June 27	22
2004	May 7/May 21	19
	May 21/June 8	10
	June 8/June 25	24
	June 25/June 27	12
2005	May 8/May 9	8
	May 9/May 11	0
	May 11/May 15	2
	May 15/May 27	12
	May 27/June 13	10
	June 13/June 28	20
2006	May 9/May 25	26
	May 25/June 13	30
	June 13/July 2	8
2007	May 14/May 29	22
	May 29/June 1	22
	June 1/June 5	30
	June 5/June 15	30
2008	May 13/May 14	4
	May 14/May 16	4
	May 16/June 2	26
	June 2/June 17	26
2009	May 15/May 17	20
	May 17/May 18	16
	May 18/June 2	26
	June 2/June 5	24
2010	June 5/June 21	6
	May 18/May 21	8
	May 21/June 4	12
	June 4/June 6	14
	June 6/June 7	24
	June 7/June 22	12

that measure relative changes in backscatter response either along the river or over time. Our results show that these relative parameters are more useful for monitoring purposes and bracketing the time of river breakup. The variance parameter (breakup indicator 2) was successful as a breakup indicator eight out of nine times. SROC served as an effective breakup indicator four out of eight times. In 2008, when variance was not useful in bracketing breakup timing, SROC turned out to be successful. Hence, combining breakup indicators 2 and 3 may increase the robustness of SAR-based river breakup analysis.

## CONCLUSIONS

Though a satellite-based monitoring system is not a substitute for site-specific, field-based observations, we conclude that time series analysis of SAR images can provide an alternative means of broadly bracketing river breakup.

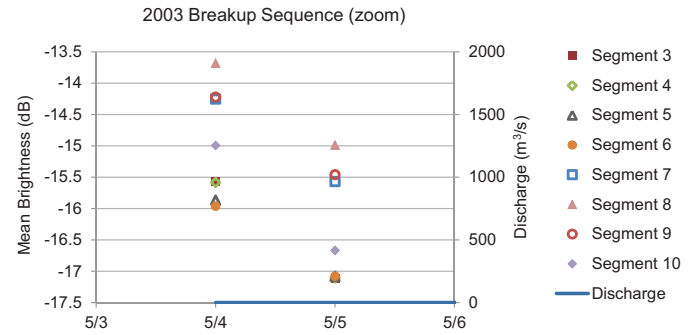


FIG. 5. Enlarged portion of the 2003 breakup sequence to reveal the similarity of the river segment brightness patterns in the SAR acquisitions from 4 May and 5 May. No river discharge was recorded on either day.

Use of SAR images is particularly suitable for large remote Arctic rivers that are often obstructed by clouds, which restrict the availability of usable optical remote sensing images for monitoring. In high latitudes, SAR images acquired from multiple satellites provide a sufficient temporal resolution even at a medium spatial resolution (~30 m), which makes them useful for monitoring narrower rivers that cannot be monitored using the coarse (500 m to 1 km) spatial resolution of MODIS and AVHRR images. The use of SAR data was most effective in bracketing the breakup period when sufficient SAR images were available to define the pre-breakup, breakup, and post-breakup periods. SAR brightness (backscatter) value, or change in brightness value over time, was not in itself a reliable indicator of breakup. However, combined use of mean backscatter variance within different segments of the river and the sum of rank order change provided a good way to bracket the breakup period.

River ice breakup is a highly complex process. For this research, river breakup was defined as the swift initial rise in discharge forming a distinctive large peak on the hydrograph after a period of dormancy during the winter months. This hydrographic peak is difficult to correlate accurately with breakup interpreted from SAR images. SAR is very sensitive to changes in the dielectric constant and to surface geometry, and it may capture changes in the surficial ice cover before any discharge is recorded on the hydrograph. This fact may lead to a discrepancy between the definitions of river ice breakup made using SAR and those made using discharge data.

Recommendations for future studies include the use of a minimum of six images per year: two pre-breakup images (ideally taken within 10 days of first recorded discharge), two acquisitions during the breakup event (based on a rapid rise in discharge recorded by the hydrograph), and two post-breakup images. More images acquired within this narrow time span are preferable and will likely result in a more refined determination of breakup onset. Additionally, wind can variably affect the overall backscatter values on the SAR images. Therefore, a general wind correction is recommended.

TABLE 4. Table showing variables used to identify the start and end dates of river breakup from 2001 to 2010. For each year, variables marked with (✓) were successful indicators, and those marked with (×) were unsuccessful. N/A indicates insufficient data for an analysis.

Year	Brightness	Variance	Sum of rank order change
2001	×	✓	×
2003	×	✓	✓
2004	×	✓	×
2005	×	✓	✓
2006	×	✓	N/A
2007	×	✓	×
2008	×	×	✓
2009	×	✓	✓
2010	×	✓	×

### ADVANTAGES AND LIMITATIONS OF STUDY

The greatest advantage of SAR is its all-weather capability, which assures data acquisition regardless of cloud cover. Between ERS-2 and RADARSAT-1 satellites, there was enough data coverage for most of the years to generate a temporal sequence of images. A time sequence of more closely spaced image acquisitions would obviously be preferable. With such a sequence, we might be able to define the breakup period more precisely, rather than broadly bracketing it as this study does.

A limitation in this study was the low spatial resolution of the SAR sensors compared to the dimensions of the river. A finer spatial resolution would probably have resulted in a more robust statistical analysis.

We recommend carrying out similar studies on other gauged Arctic rivers to add to the present state of knowledge. Supplementing the satellite image data sets with carefully timed airborne image acquisitions close to the breakup time will help us tremendously both to understand the breakup process and to refine the data processing and analysis strategy for determining breakup timing.

### ACKNOWLEDGEMENTS

This work would not have been possible without generous support from the Alaska Satellite Facility, the University of Alaska Fairbanks Geophysical Institute, the Scenarios Network for Alaska and Arctic Planning, the Alaska Climate Science Center, NASA's Alaska EPSCoR program, and the Department of Geology and Geophysics, University of Alaska Fairbanks.

### REFERENCES

Best, H., McNamara, J.P., and Liberty, L. 2005. Association of ice and river channel morphology determined using ground-penetrating radar in the Kuparuk River, Alaska. *Arctic, Antarctic, and Alpine Research* 37(2):157–162.  
[http://dx.doi.org/10.1657/1523-0430\(2005\)037%5B0157:AOIARC%5D2.0.CO;2](http://dx.doi.org/10.1657/1523-0430(2005)037%5B0157:AOIARC%5D2.0.CO;2)

Bring, A., and Destouni, G. 2009. Hydrological and hydrochemical observation status in the pan-Arctic drainage basin. *Polar Research* 28(3):327–338.  
<http://dx.doi.org/10.3402/polar.v28i3.6140>

Broecker, W.S. 1997. Thermohaline circulation, the Achilles Heel of our climate system: Will man-made CO<sub>2</sub> upset the current balance? *Science* 278(5343):1582–1588.  
<http://dx.doi.org/10.1126/science.278.5343.1582>

Floyd, A., Gens, R., Prakash, A., Meyer, F., and Liljedahl, A.K. 2012. Using synthetic aperture radar to study river ice breakup on the Kuparuk River, northern Alaska. American Water Resource Association, Alaska Section Annual Conference, 5–7 March 2012, Juneau, Alaska.  
<http://state.awra.org/alaska/2012awra-ak-final.pdf>

Gauthier, Y., Weber, F., Savary, S., Jasek, M., Paquet, L.-M., and Bernier, M. 2006. A combined classification scheme to characterise river ice from SAR data. *Proceedings of European Association of Remote Sensing Laboratories (EARSeL)* 5:77–88.

Gauthier, Y., Tremblay, M., Bernier, M., and Furgal, C. 2010. Adaptation of a radar-based river ice mapping technology to the Nunavik context. *Canadian Journal of Remote Sensing* 36(S1):S168–S185.  
<http://dx.doi.org/10.5589/m10-018>

Gens, R., and Logan, T. 2003. Alaska Satellite Facility software tools: Manual. Fairbanks: Geophysical Institute, University of Alaska Fairbanks. 180 p.

Horstmann, J., Schiller, H., Schulz-Stellenfleth, J., and Lehner, S. 2003. Global wind speed retrieval from SAR. *IEEE Transactions on Geoscience and Remote Sensing* 41(10):2277–2286.  
<http://dx.doi.org/10.1109/TGRS.2003.814658>

Jasek, M., Weber, F., and Hurley, J. 2003. Ice thickness and roughness analysis on the Peace River using RADARSAT-1 SAR imagery. 12th Workshop on the Hydraulics of Ice Covered Rivers, Canadian Geophysical Union Hydrology Section (CGU HS) Committee on River Ice Processes and the Environment, 19–20 June 2003, Edmonton, Alberta. 50–68.

Jeffries, M.O., Morris, K., and Kozlenko, N. 2005. Ice characteristics and processes, and remote sensing of frozen rivers and lakes. In: Duguay, C.R., and Pietroniro, A., eds. *Remote sensing in northern hydrology: Measuring environmental change*. Geophysical Monograph 163. Washington, D.C.: American Geophysical Union. 63–90.  
<http://dx.doi.org/10.1029/163GM05>

Kane, D.L., and Hinzman, L.D. 2012. Climate data from the North Slope Hydrology Research project. Fairbanks: Water and Environmental Research Center, University of Alaska Fairbanks.  
[http://ine.uaf.edu/werc/projects/NorthSlope/upper\\_kuparuk/uk\\_river/uk\\_river.html](http://ine.uaf.edu/werc/projects/NorthSlope/upper_kuparuk/uk_river/uk_river.html)

Kane, D.L., Hinzman, L.D., Benson, C.S., and Liston, G.E. 1991. Snow hydrology of a headwater Arctic Basin. 1. Physical measurements and process studies. *Water Resources Research* 27(6):1099–1109.  
<http://dx.doi.org/10.1029/91WR00262>

- Kane, D.L., Gieck, R.E., and Hinzman, L.D. 1997. Snowmelt modeling at small Alaskan Arctic watershed. *Journal of Hydrologic Engineering* 2(4):204–210.  
[http://dx.doi.org/10.1061/\(ASCE\)1084-0699\(1997\)2:4\(204\)](http://dx.doi.org/10.1061/(ASCE)1084-0699(1997)2:4(204))
- Kane, D.L., Hinzman, L.D., McNamara, J.P., Zhang, Z., and Benson, C.S. 2000. An overview of a nested watershed study in Arctic Alaska. *Nordic Hydrology* 31(4-5):245–266.  
<http://dx.doi.org/10.2166/nh.2000.015>
- Kane, D.L., McNamara, J.P., Yang, D., Olsson, P.Q., and Gieck, R.E. 2003. An extreme rainfall/runoff event in Arctic Alaska. *Journal of Hydrometeorology* 4(6):1220–1228.  
[http://dx.doi.org/10.1175/1525-7541\(2003\)004%3C1220:AEREIA%3E2.0.CO;2](http://dx.doi.org/10.1175/1525-7541(2003)004%3C1220:AEREIA%3E2.0.CO;2)
- Kane, D.L., Hinzman, L.D., Gieck, R.E., McNamara, J.P., Youcha, E.K., and Oatley, J.A. 2008. Contrasting extreme runoff events in areas of continuous permafrost, Arctic Alaska. *Hydrology Research* 39(4):287–298.  
<http://dx.doi.org/10.2166/nh.2008.005>
- Liljedahl, A.K., Hinzman, L.D., Harazono, Y., Zona, D., Tweedie, C.E., Hollister, R.D., Engstrom, R., and Oechel, W.C. 2011. Nonlinear controls on evapotranspiration in Arctic coastal wetlands. *Biogeosciences* 8:3375–3389.  
<http://dx.doi.org/10.5194/bg-8-3375-2011>
- McNamara, J.P., Kane, D.L., and Hinzman, L.D. 1998. An analysis of streamflow hydrology in the Kuparuk River Basin, Arctic Alaska: A nested watershed approach. *Journal of Hydrology* 206(1-2):39–57.  
[http://dx.doi.org/10.1016/S0022-1694\(98\)00083-3](http://dx.doi.org/10.1016/S0022-1694(98)00083-3)
- Mermoz, S., Allain, S., Bernier, M., Pottier, E., and Gherboudj, I. 2009. Classification of river ice using polarimetric SAR data. *Canadian Journal of Remote Sensing* 35(5):460–473.  
<http://dx.doi.org/10.5589/m09-034>
- Mermoz, S., Allain, S., Bernier, M., Pottier, E., Van der Sanden, J.J., and Chokmani, K. 2012. Retrieval of river ice thickness from C-band PolSAR data. 2012 IEEE International Geoscience & Remote Sensing Symposium (IGARSS), 22–27 July 2012, Munich, Germany. 3237–3240.  
<http://dx.doi.org/10.1109/IGARSS.2012.6350734>
- Osterkamp, T.E., and Payne, M.W. 1981. Estimates of permafrost thickness from well logs in northern Alaska. *Cold Regions Science and Technology* 5(1):13–27.  
[http://dx.doi.org/10.1016/0165-232X\(81\)90037-9](http://dx.doi.org/10.1016/0165-232X(81)90037-9)
- Peterson, B.J., Holmes, R.M., McClelland, J.W., Vörösmarty, C.J., Lammers, R.B., Shiklomanov, A.I., Shiklomanov, I.A., and Rahmstorf, S. 2002. Increasing river discharge to the Arctic Ocean. *Science* 298(5601):2171–2173.  
<http://dx.doi.org/10.1126/science.1077445>
- Prowse, T.D., and Beltaos, S. 2002. Climatic control of river-ice hydrology: A review. *Hydrological Processes* 16(4):805–822.  
<http://dx.doi.org/10.1002/hyp.369>
- Prowse, T.D., Wrona, F.J., Reist, J.D., Gibson, J.J., Hobbie, J.E., Lévesque, L.M.J., and Vincent, W.F. 2006. Climate change effects on hydroecology of Arctic freshwater ecosystems. *AMBIO: A Journal of the Human Environment* 35(7):347–358.  
[http://dx.doi.org/10.1579/0044-7447\(2006\)35%5B347:CCEOH0%5D2.0.CO;2](http://dx.doi.org/10.1579/0044-7447(2006)35%5B347:CCEOH0%5D2.0.CO;2)
- Rahmstorf, S. 2002. Ocean circulation and climate during the past 120,000 years. *Nature* 419:207–214.  
<http://dx.doi.org/10.1038/nature01090>
- Rees, W.G. 2006. Remote sensing of snow and ice. Boca Raton, Florida: CRC Press. 285 p.
- Rovaneck, R.J., Hinzman, L.D., and Kane, D.L. 1996. Hydrology of a tundra wetland complex on the Alaskan Arctic Coastal Plain, U.S.A. *Arctic and Alpine Research* 28(3):311–317.  
<http://dx.doi.org/10.2307/1552110>
- Searcy, C., Dean, K., and Stringer, W. 1996. A river-coastal sea ice interaction model: Mackenzie River Delta. *Journal of Geophysical Research* 101(C4):8885–8894.  
<http://dx.doi.org/10.1029/96JC00120>
- Shiklomanov, N.I., and Nelson, F.E. 2002. Active-layer mapping at regional scales: A 13-year spatial time series for the Kuparuk region, north-central Alaska. *Permafrost and Periglacial Processes* 13(3):219–230.  
<http://dx.doi.org/10.1002/ppp.425>
- Steele, M., Thomas, D., Rothrock, D., and Martin, S. 1996. A simple model study of the Arctic Ocean freshwater balance, 1979–1985. *Journal of Geophysical Research* 101(C9):20833–20848.  
<http://dx.doi.org/10.1029/96JC01686>
- Unterschultz, K.D., Van der Sanden, J., and Hicks, F.E. 2009. Potential of RADARSAT-1 for the monitoring of river ice: Results of a case study on the Athabasca River at Fort McMurray, Canada. *Cold Regions Science and Technology* 55(2):238–248.  
<http://dx.doi.org/10.1016/j.coldregions.2008.02.003>
- USGS (U.S. Geological Survey). 2012. USGS 15896000 Kuparuk R near Deadhorse AK.  
[http://waterdata.usgs.gov/nwis/nwisman/?site\\_no=15896000&agency\\_cd=USGS](http://waterdata.usgs.gov/nwis/nwisman/?site_no=15896000&agency_cd=USGS)
- Van Zyl, J.J., and Kim, Y. 2011. Synthetic aperture radar polarimetry, Vol. 2. Hoboken, New Jersey: John Wiley & Sons.
- Weber, F., Nixon, D., and Hurley, J. 2003. Semi-automated classification of river ice types on the Peace River using RADARSAT-1 synthetic aperture radar (SAR) imagery. *Canadian Journal of Civil Engineering* 30(1):11–27.  
<http://dx.doi.org/10.1139/102-073>
- Weeks, W.F., Fountain, A.J., Bryan, M.L., and Elachi, C. 1978. Differences in radar returns from ice-covered North Slope lakes. *Journal of Geophysical Research* 83(C8):4069–4073.  
<http://dx.doi.org/10.1029/JC083iC08p04069>
- Yoshikawa, K., Hinzman, L.D., and Kane, D.L. 2007. Spring and aufeis (icing) hydrology in Brooks Range, Alaska. *Journal of Geophysical Research* 112, G04S43.  
<http://dx.doi.org/10.1029/2006JG000294>
- Zhang, T., Osterkamp, T.E., and Starnes, K. 1996. Some characteristics of the climate in northern Alaska, U.S.A. *Arctic and Alpine Research* 28(4):509–518.  
<http://dx.doi.org/10.2307/1551862>